Journal of Zhejiang University-SCIENCE A (Applied Physics & Engineering)
ISSN 1673-565X (Print); ISSN 1862-1775 (Online)
www.zju.edu.cn/jzus; www.springerlink.com
E-mail: jzus@zju.edu.cn

# Numerical investigation and design of thin-walled complex section steel columns*

Su-qing HUANG[1], Ju CHEN[†‡2], Wei-liang JIN[2]

([1]*Department of Civil Engineering, Zhejiang College of Construction, Hangzhou 311200, China*)

([2]*Department of Civil Engineering, Zhejiang University, Hangzhou 310058, China*)

[†]E-mail: cecj@zju.edu.cn

Received Apr. 19, 2010; Revision accepted June 8, 2010; Crosschecked Jan. 7, 2011

**Abstract:** A numerical investigation of thin-walled complex section steel columns with intermediate stiffeners was performed using finite element analysis. An accurate and reliable finite element model was developed and verified against test results. Verification indicates that the model could predict the ultimate strengths and failure modes of the tested columns with reasonable accuracy. Therefore, the developed model was used for the parametric study. In addition, the effect of geometric imperfection on column ultimate strength and the effect of boundary conditions on the elastic distortional buckling of complex section columns were investigated. An equation for the elastic distortional buckling load of fixed-ended columns having different column lengths was proposed. The elastic distortional buckling load obtained from the proposed equation was used in the direct strength method to calculate the column ultimate strength. Generally, it is shown that the proposed design equation conservatively predicted the ultimate strengths of complex section columns with different column lengths.

**Key words:** Complex section column, Distortional buckling, Finite element method (FEM), Intermediate stiffener
**doi:**10.1631/jzus.A1000185 **Document code:** A **CLC number:** TU391

## 1 Introduction

Thin-walled cold-formed steel sections have been used increasingly in recent years. There are some advantages in using cold-formed steel as a structural material, such as high strength-to-weight ratio and ease of production. However, one disadvantage is that large width-to-thickness ratio sections can suffer a loss of strength in a localized region when 2D plate buckling occurs, known as local buckling (Yu, 2000). Previous research indicated that stiffeners have significant effects on local buckling stress (Yan and Young, 2002; Young and Yan, 2004b). Therefore, a new section with intermediate stiffeners in the web was proposed (Young and Chen, 2008). An experimental investigation was carried out on the complex section steel column with intermediate stiffeners. The details of the test program are presented in Chen *et al*. (2010). In this study, a numerical parametric study is conducted to further investigate the behavior and ultimate strengths of complex section columns with intermediate stiffeners. The finite element program ABAQUS (2004) has been widely used to investigate the behavior of cold-formed steel columns (Kaitila, 2002; Young, 2004; Young and Yan, 2004a; Chen and Young, 2007; Young and Ellobody, 2007). Therefore, the finite element program ABAQUS was used to simulate the complex section columns in this study.

The direct strength method (DSM), specified in the supplement to the North American Specification (AISI, 2004), proposed by Schafer and Peköz (1998), is based on the same underlying empirical assumption as the effective width method: ultimate strength is a function of the elastic buckling and the yielding of the

‡ Corresponding author

* Project supported by the Department of Education of Zhejiang Province (No. Y200804537), the Zhejiang University Zijin Project, and the Zhejiang College of Construction (No. 200914), China

material (Schafer, 2002). Recent research on the application of the DSM on cold-formed steel structures has also been reported (Sputo and Tovar, 2005; Tovar and Sputo, 2005; Yu and Schafer, 2007; Kwon *et al*., 2009; Dawe *et al*., 2010). However, the DSM emphasizes the use of finite strip analysis for the determination of elastic buckling. Finite strip analysis is a general tool that provides accurate elastic buckling solutions with a minimum of effort and time. Finite strip analysis, as implemented in conventional programs, does have limitations: it provides a solution for member ends which are pinned only (AISI, 2006). Previous research has indicated that distortional buckling can be influenced by additional restraint provided at the ends, but no direct way exists to capture this effect in a traditional finite strip analysis (AISI, 2006). The buckling mode of the proposed complex section is general distortional buckling; therefore, the effect of boundary conditions on the distortional buckling of complex section fixed-ended columns was investigated.

The purpose of this study is firstly to develop an accurate finite element model to investigate the behavior of complex section columns with intermediate stiffeners. Secondly, a comparison of the ultimate column strengths from the finite element analysis (FEA) and DSM predictions were made. A design method for the elastic distortional buckling of fixed-ended complex section columns is also proposed.

## 2 Test program

The test program conducted by Chen *et al*. (2010) provided experimental ultimate strengths and failure modes of complex section stub columns compressed between fixed ends. The test specimens were brake-pressed from thin-walled structural steel sheets. The minimal column length of each specimen was about 400 mm. The ends of the specimen were then welded to 10 mm thick steel plates to ensure full contact between the specimen and the end bearings. The nominal cross section dimensions of specimens are shown in Table 1 and Fig. 1. The specimens are labeled according to their cross sections and column lengths. For example, "S1L400A" defines the specimens as follows: (1) The first two letters indicate the section type of the specimen. (2) The third letter "L" refers to the column length. (3) The following three or four digits are the nominal specimen length (400 mm). (4) The last letter "A" or "B" means repeated test of the same section.

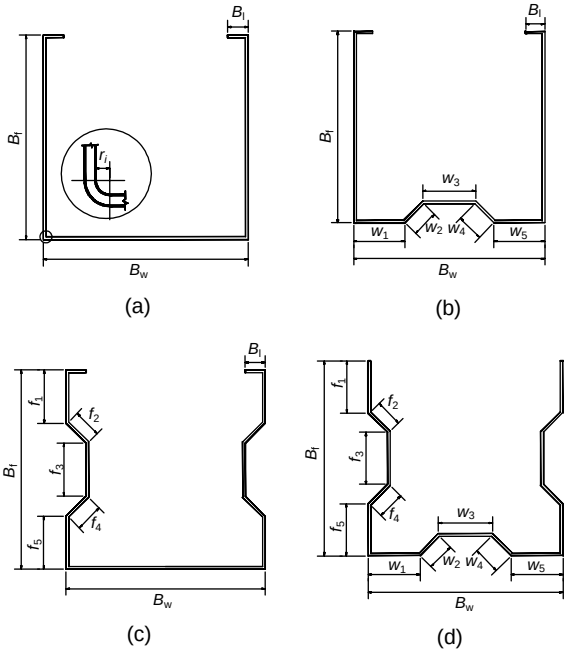


**Fig. 1 Cross sections of test specimens (Chen *et al*., 2010)**
(a) Section 1; (b) Section 2; (c) Section 3; (d) Section 4

**Table 1 Measured dimension of test specimens (Chen *et al*., 2010)**

| Specimen | Length (mm) | Thickness (mm) | Lip (mm) | Flange (mm) | | | | | | Web (mm) | | | | | |
|---|---|---|---|---|---|---|---|---|---|---|---|---|---|---|---|
| | $L$ | $t$ | $B_l$ | $B_f$ | $f_1$ | $f_2$ | $f_3$ | $f_4$ | $f_5$ | $B_w$ | $w_1$ | $w_2$ | $w_3$ | $w_4$ | $w_5$ |
| S1L400A | 401.0 | 1.98 | 14.9 | 149.6 | – | – | – | – | – | 149.5 | – | – | – | – | – |
| S1L400B | 400.0 | 1.99 | 14.8 | 149.5 | – | – | – | – | – | 149.6 | – | – | – | – | – |
| S2L400A | 400.0 | 1.98 | 15.0 | 150.0 | – | – | – | – | – | 151.0 | 40 | 22 | 40 | 22 | 40 |
| S2L400B | 399.8 | 2.00 | 14.9 | 150.0 | – | – | – | – | – | 151.0 | 40 | 22 | 40 | 22 | 40 |
| S3L400A | 400.5 | 2.00 | 15.0 | 149.3 | 40 | 22 | 40 | 22 | 40 | 151.1 | – | – | – | – | – |
| S3L400B | 400.0 | 1.98 | 14.8 | 149.5 | 40 | 22 | 40 | 22 | 40 | 151.3 | – | – | – | – | – |
| S4L400A | 399.5 | 2.00 | – | 150.2 | 40 | 22 | 40 | 22 | 40 | 151.4 | 40 | 22 | 40 | 22 | 40 |
| S4L400B | 400.8 | 2.00 | – | 150.2 | 40 | 22 | 40 | 22 | 40 | 152.6 | 40 | 22 | 40 | 22 | 40 |

The material properties of test specimens were measured by tensile coupon tests (Table 2). The details of the experimental investigation are presented in (Chen *et al*., 2010).

**Table 2 Measured material properties obtained from tensile coupon tests (Chen *et al*., 2010)**

| Specimen | $E$ (GPa) | $\sigma_y$ (MPa) | $\sigma_u$ (MPa) |
|---|---|---|---|
| Steel sheet | 204 | 401 | 520 |
| Cold-formed specimen | 210 | 413 | 528 |

$E$: elastic modulus; $\sigma_y$: yield strength; $\sigma_u$: ultimate strength

## 3 Finite element model

The finite element program ABAQUS (2004) was used in the simulation of complex section fixed-ended columns with intermediate stiffeners tested by Chen et al. (2010). The measured geometry and initial geometric imperfections were incorporated in the finite element model. The simulation consisted of two steps. The first was eigenvalue analysis to determine the buckling modes, and the second was load-displacement nonlinear analysis (ABAQUS, 2004).

The four-node doubly curved shell element with reduced integration and hourglass control (S4R5) was used in the model. Convergence studies were conducted to choose the reasonable finite element mesh, and finally, a 10 mm×10 mm (length by width) size was used in modeling the test columns. The fixed-ended boundary condition and loading application were simulated as described in (Chen and Young, 2007).

The measured material properties were used in the finite element model. The true stresses and true plastic strains were used in the material model. Details of the imperfection measurement are reported in (Chen *et al*., 2010).

## 4 Test verification

The FEA results were verified against the test results. As shown in Table 3, the FEA results ($P_{FEA}$) agree with test results ($P_{EXP}$) well. The $P_{FEA}$ are slightly higher than $P_{EXP}$, except for the specimens S3L400A and S3L400B. The mean value of the $P_{EXP}/P_{FEA}$ ratio is 0.98 with the corresponding coefficient of variation (COV) of 0.031. The comparison indicates that the developed finite element model is accurate and reliable.

**Table 3 Compressive strengths and failure modes of test specimens**

| Specimen | Test | | FEA | | $P_{EXP}/P_{FEA}$ |
|---|---|---|---|---|---|
| | $P_{EXP}$ (kN) | Failure mode | $P_{FEA}$ (kN) | Failure mode | |
| S1L400A | 173 | D | 175 | D | 0.99 |
| S1L400B | 175 | D | 176 | D | 0.99 |
| S2L400A | 232 | D | 252 | D | 0.92 |
| S2L400B | 243 | D | 253 | D | 0.96 |
| S3L400A | 342 | D | 340 | D | 1.01 |
| S3L400B | 347 | D | 340 | D | 1.02 |
| S4L400A | 344 | D | 347 | D | 0.99 |
| S4L400B | 342 | D | 347 | D | 0.99 |
| Mean | | | | | 0.98 |
| COV | | | | | 0.031 |

D: distortional buckling; COV: coefficient of variation

The failure modes of each specimen from the FEA and the tests are also compared in Table 3. It can be seen that the failure modes from FEA and the tests are all distortional buckling. The deformed shape obtained from the FEA was compared with the test specimen (Fig. 2). The load-displacement curves of the specimen S4L400B from the FEA and test are compared in Fig. 3, and it is shown that the finite element model is able to predict the load-displacement curve with reasonable accuracy.

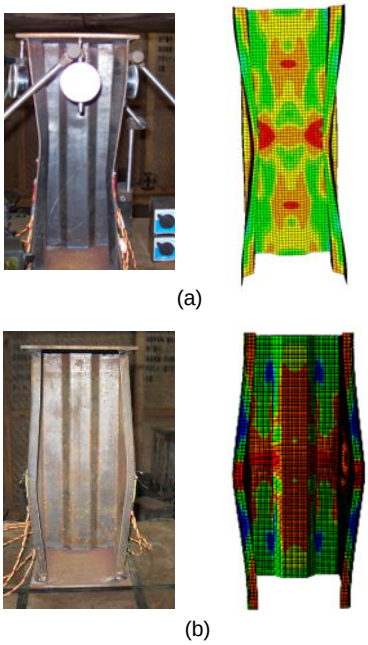


**Fig. 2 Comparison of failure modes**
(a) Local buckling; (b) Distortional buckling

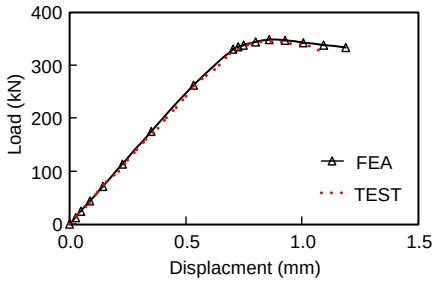


**Fig. 3 Comparison of load-displacement curves**

## 5 Parametric study

### 5.1 General

The developed finite element model was used in the parametric study. The overall imperfection magnitude was 1/1000 of the column length. The size of the finite element mesh for all columns was almost 10 mm×10 mm (length by width). The measured material properties were also used in the parametric study.

### 5.2 Effect of different initial local imperfection

The effect of initial geometry imperfection on the FEA model of column with intermediate stiffeners was investigated. As shown in Fig. 4, the effect of initial local geometry imperfection on load-bearing capacity decreases from section 1 to section 4. It may indicate that for more complex sections, the effect of initial local geometry imperfection is smaller.

### 5.3 Effect of buckling deformation shape

Eigenvalues of the corresponding buckling mode are used to obtain the distortional buckling stress in the FEA. Normally the distortional buckling mode has two different deformation shapes, i.e., deformation of lips in the outward and inward directions. In this study, the elastic distortional buckling loads of lip inward deformation ($P_{\text{crd-in}}$) and lip outward deformation ($P_{\text{crd-out}}$) were compared (Table 4), and were similar for specimens with different buckling deformation shapes.

### 5.4 Effect of boundary condition on distortional buckling

The elastic distortional buckling loads ($P_{\text{crd-FEA}}$) of columns having different lengths were obtained using eigenvalue analysis. The analysis results are

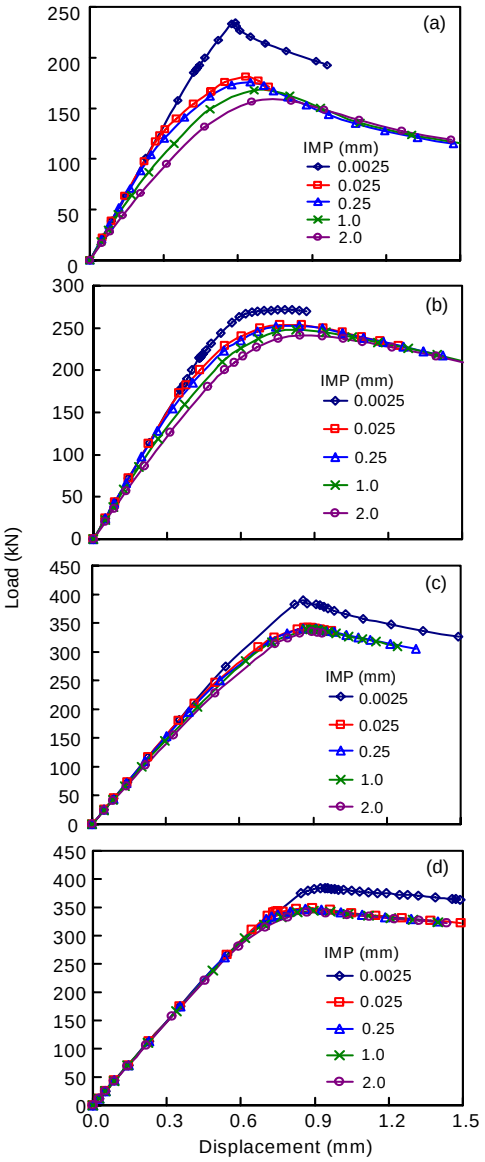


**Fig. 4 Imperfection sensitivity analysis of complex column sections**

(a) Section 1; (b) Section 2; (c) Section 3; (d) Section 4. IMP: initial local geometry imperfection, mm

**Table 4 Effect of deformation shapes on the buckling load in the FEA**

| Specimen | $P_{\text{crd-in}}$ (kN) | $P_{\text{crd-out}}$ (kN) |
|---|---|---|
| S1L400A | 169.6 | 175.3 |
| S2L400A | 199.7 | 201.8 |
| S3L400A | 744.8 | 766.3 |
| S4L400A | 352.7 | 365.4 |

$P_{\text{crd-in}}$ and $P_{\text{crd-out}}$ are the elastic distortional buckling loads of the lip inward deformation and outward deformation, respectively

compared with elastic buckling load obtained from the finite strip method (FSM) ($P_{\text{crd-FSM}}$) (Papangelis and Hancock, 1995) (Table 5). The comparison indicates that the elastic distortional buckling load obtained from the FEA decreases when the column length increases. It is also shown that the elastic distortional buckling load obtained from the FEA approaches that obtained from the FSM when the column length increases. The load ratio of $P_{\text{crd-FEA}}/P_{\text{crd-FSM}}$ is plotted against the number of distortional half-waves along the column length ($\lambda$) in Fig. 5. The distortional half-wave length is obtained from the FSM. It is shown that the load ratio of $P_{\text{crd-FEA}}/P_{\text{crd-FSM}}$ for different sections could fit a single curve when the number of distortional half-waves along the column length is larger than 1. When the number of distortional half-waves along column length is smaller than 1, the load ratio of $P_{\text{crd-FEA}}/P_{\text{crd-FSM}}$ are different for different sections.

**Table 5 Elastic distortional buckling load obtained from numerical analysis**

| Method | Length (mm) | Distortional buckling load, $P_{\text{crd}}$ (kN) | | | |
|---|---|---|---|---|---|
| | | Section 1 | Section 2 | Section 3 | Section 4 |
| FEA | 400 | 169.6 | 199.7 | 744.8 | 352.7 |
| | 500 | 153.3 | 180.4 | 565.6 | 305.7 |
| | 600 | 141.0 | 166.9 | 426.8 | 275.9 |
| | 700 | 131.3 | 151.4 | 301.7 | 252.4 |
| | 800 | 121.5 | 137.1 | 289.6 | 231.9 |
| | 900 | 113.0 | 126.0 | 250.0 | 214.5 |
| | 1000 | 107.8 | 118.8 | 216.6 | 200.9 |
| | 1500 | 99.5 | 108.7 | 171.1 | 174.6 |
| | 2000 | 89.2 | 97.0 | 157.2 | 159.6 |
| | 2500 | 86.9 | 94.5 | 142.4 | 150.8 |
| | 3000 | 84.2 | 92.4 | 136.6 | 139.9 |
| FSM | – | 83.8 | 92.0 | 135.1 | 137.4 |

The equation for the effect of fixed-ended boundary conditions on the distortional buckling was proposed in the DSM guide manual (AISI, 2006), and is shown as

$$\frac{P_{\text{crd-FEA}}}{P_{\text{crd-FSM}}}=1+\frac{0.6}{\lambda^{1.5}}, \tag{1}$$

from which the prediction was compared with the numerical results obtained in this study (Fig. 5). Note that Eq. (1) is proposed for the number of distortional half-waves along the column length equal to or larger than 1. The comparison indicates that the predictions from Eq. (1) are generally non-conservative. Therefore, a modified equation was proposed:

$$\frac{P_{\text{crd-FEA}}}{P_{\text{crd-FSM}}}=1+\frac{0.3}{\lambda^{1.5}}, \tag{2}$$

and it is shown that the equation curve is generally the lower boundary of all the data.

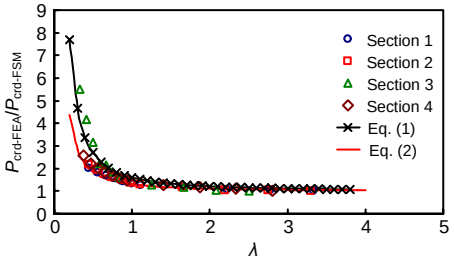


**Fig. 5 Effect of the number of distortional half-waves along the length on the elastic distortional buckling load**

### 5.5 Effect of different column lengths

As shown in Fig. 6, the ultimate strengths of the columns decrease when the column lengths increase from 400 to 1000 mm. It is shown that the ultimate strengths of column sections 1 and 2 almost remain constant when the column length increases from 1000 to 3000 mm. For column sections 3 and 4, the ultimate strengths slightly decrease when the column lengths increase from 1000 to 2500 mm.

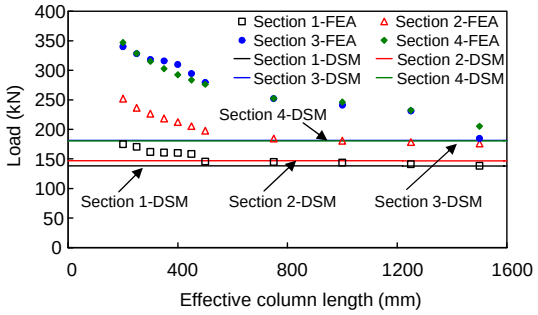


**Fig. 6 Ultimate strengths of the columns with different column lengths**

## 6 Design rules

### 6.1 General

As recommended by Young and Rasmussen (1998), the effective lengths ($l_e$) for the major axis ($l_{ex}$) and the minor axis ($l_{ey}$) flexural buckling as well

as torsional buckling ($l_{ez}$) are assumed to be equal to half of the column length ($L$) for the fixed-ended concentrically-loaded columns in the design.

### 6.2 Comparison of FEA results with design predictions

The DSM is used to predict the strengths of complex section columns with intermediate stiffeners as follows:

$$P_{DSM}=\min(P_{ne}, P_{nl}, P_{nd}), \tag{3}$$

$$P_{ne}=\begin{cases}\left(0.658^{\lambda_c^2}\right)P_y, & \lambda_c \le 1.5,\\ \left(\dfrac{0.877}{\lambda_c^2}\right)P_y, & \lambda_c > 1.5,\end{cases} \tag{4}$$

$$P_{nl}=\begin{cases}P_{ne}, & \lambda_l \le 0.776,\\ \left[1-0.15\left(\dfrac{P_{crl}}{P_{ne}}\right)^{0.4}\right]\left(\dfrac{P_{crl}}{P_{ne}}\right)^{0.4}P_{ne}, & \lambda_l > 0.776,\end{cases} \tag{5}$$

$$P_{nd}=\begin{cases}P_y, & \lambda_d \le 0.561,\\ \left[1-0.25\left(\dfrac{P_{crd}}{P_y}\right)^{0.6}\right]\left(\dfrac{P_{crd}}{P_y}\right)^{0.6}P_y, & \lambda_d > 0.561,\end{cases} \tag{6}$$

where $P_y=f_yA_g$, $P_{cre}=\pi^2EA/(l_e/r)^2$, $\lambda_c=\sqrt{P_y/P_{cre}}$, $\lambda_l=\sqrt{P_{ne}/P_{crl}}$, $\lambda_d=\sqrt{P_y/P_{crd}}$. $P_{cre}$ is the critical elastic buckling load in flexural buckling. $P_{ne}$ is the nominal axial strength for flexural, torsional, or flexural-torsional buckling, and $P_{nl}$ and $P_{nd}$ are the nominal axial strengths for local buckling and distortional buckling, respectively. $P_y$ is the nominal section yield strength. $f_y$ is the material yield strength, which is the static 0.2% proof stress ($\sigma_{0.2}$). $P_{crl}$ and $P_{crd}$ are the critical elastic buckling loads for the local columns and distortional columns, respectively. $\lambda_c$, $\lambda_d$, and $\lambda_l$ are the slendernesses of the overall buckling, distortional buckling, and local buckling, respectively. $A$ is the cross section area, $A_g$ is the full cross section area, $E$ is the elastic modulus, and $r$ is the radius of gyration of gross cross section about the minor $y$-axis of buckling.

The ultimate strengths predicted by the DSM with $P_{crl}$ and $P_{crd}$ calculated using the FSM (Papangelis and Hancock, 1995) were compared with the FEA parametric study results (Fig. 6). Since the ultimate strengths calculated by Eq. (6) have no relationship with the column length, the design curves are all horizontal straight lines. It is shown that the ultimate strengths predicted by the DSM are very conservative for column sections 2, 3, and 4. The current DSM was developed based on open sections rather than complex sections. Hence, the predictions of the DSM on the complex sections may differ from those of simple channel sections.

The ultimate strengths ($P_{DSM\text{-}M}$) predicted using the DSM with $P_{crd}$ calculated by Eq. (2) were compared with the FEA parametric study results in Table 6.

**Table 6 Comparison of the column strengths of the sections from the FEA with the DSM predictions**

| Length (mm) | Section 1 | | | Section 2 | | | Section 3 | | | Section 4 | | |
|---|---|---|---|---|---|---|---|---|---|---|---|---|
| | $P_{FEA}$ (kN) | $P_{DSM\text{-}M}$ (kN) | Ratio | $P_{FEA}$ (kN) | $P_{DSM\text{-}M}$ (kN) | Ratio | $P_{FEA}$ (kN) | $P_{DSM\text{-}M}$ (kN) | Ratio | $P_{FEA}$ (kN) | $P_{DSM\text{-}M}$ (kN) | Ratio |
| 400 | 176.0 | 195.7 | 0.90 | 252.0 | 210.5 | 1.20 | 340.0 | 264.5 | 1.29 | 347.0 | 267.8 | 1.30 |
| 500 | 170.4 | 183.1 | 0.93 | 236.6 | 195.0 | 1.21 | 328.0 | 260.3 | 1.26 | 328.7 | 247.9 | 1.33 |
| 600 | 165.0 | 173.5 | 0.95 | 226.7 | 184.8 | 1.23 | 318.1 | 244.8 | 1.30 | 315.0 | 234.3 | 1.34 |
| 700 | 160.8 | 166.9 | 0.96 | 218.4 | 177.7 | 1.23 | 316.0 | 233.7 | 1.35 | 302.7 | 224.7 | 1.35 |
| 800 | 159.3 | 162.0 | 0.98 | 212.5 | 172.6 | 1.23 | 309.7 | 225.5 | 1.37 | 292.4 | 217.5 | 1.34 |
| 900 | 156.7 | 158.4 | 0.99 | 205.4 | 168.7 | 1.22 | 294.7 | 219.2 | 1.34 | 283.6 | 212.1 | 1.34 |
| 1000 | 151.2 | 155.6 | 0.97 | 197.7 | 165.7 | 1.19 | 279.7 | 214.2 | 1.31 | 276.2 | 207.8 | 1.33 |
| 1500 | 144.7 | 147.9 | 0.98 | 184.7 | 157.4 | 1.17 | 252.0 | 200.1 | 1.26 | 252.5 | 195.9 | 1.29 |
| 2000 | 143.8 | 144.5 | 1.00 | 180.7 | 153.7 | 1.18 | 241.0 | 193.8 | 1.24 | 246.3 | 190.6 | 1.29 |
| 2500 | 141.1 | 142.7 | 0.99 | 178.5 | 151.8 | 1.18 | 231.3 | 190.4 | 1.21 | 232.5 | 187.7 | 1.24 |
| 3000 | 138.4 | 141.6 | 0.98 | 176.1 | 150.6 | 1.17 | 184.7 | 188.3 | 0.98 | 205.3 | 185.9 | 1.10 |
| Mean | | | 0.97 | | | 1.20 | | | 1.27 | | | 1.30 |
| COV | | | 0.030 | | | 0.020 | | | 0.084 | | | 0.055 |

COV: coefficient of variation; ratio: $P_{FEA}/P_{DSM\text{-}M}$

It is shown that the ultimate strengths predicted by the DSM generally agree with the FEA results well for column series section 1. The mean value of the $P_{FEA}/P_{DSM\text{-}M}$ ratio is 0.97 with the corresponding COV being 0.030. For column series sections 2, 3, and 4, the DSM predictions are all conservative. The mean values of the $P_{FEA}/P_{DSM\text{-}M}$ ratio for column series are 1.20, 1.27, and 1.30, with the corresponding COV of 0.020, 0.084, and 0.055, respectively.

## 7 Conclusions

Numerical investigations and design of fixed-ended complex section columns using the FEA have been presented. A finite element model, including geometric and material nonlinearities, has been developed and verified against experimental results. The FEA predictions were generally in good agreement with the experimental ultimate strengths and failure modes of the test columns. The columns underwent distortional buckling. An extensive parametric study of initial geometric imperfection, buckling deformation shape, boundary condition, and column length effects on elastic distortional buckling load has been performed using the developed finite element model. It is shown that for more complex sections, the effect of initial local geometry imperfection is smaller. The buckling deformation shape has no significant effect on the buckling load. It is also shown that the elastic distortional buckling load of a column obtained from the FEA approached that obtained from the FSM when the column lengths increases. A comparison of the column strengths obtained from the FEA and the design column strengths calculated using the DSM has also been presented. Results showed that the design column strengths calculated using the critical elastic distortional buckling load obtained from the proposed equation were generally conservative for fixed-ended complex section columns.

## References


ABAQUS, 2004. Analysis User's Manual. Version 6.5. ABAQUS, Inc.

AISI (American Iron and Steel Institute), 2004. Supplement to the North American Specification for Design of Cold-Formed Steel Structural Members. AISI, Washington, DC.

AISI (American Iron and Steel Institute), 2006. Direct Strength Method Design Guide. AISI, Washington, DC.

Chen, J., Young, B., 2007. Cold-formed steel lipped channel columns at elevated temperatures. *Engineering Structures*, **29**(10):2445-2456. [doi:10.1016/j.engstruct.2006.12.004]

Chen, J., Yong, H., Jin, W.L., 2010. Stub column tests of thin-walled complex section with intermediate stiffeners. *Thin-Walled Structures*, **48**(6):423-429. [doi:10.1016/j.tws.2010.01.008]

Dawe, J.L., Liu, L., Li, J.Y., 2010. Strength and behavior of cold-formed steel offset trusses. *Journal of Constructional Steel Research*, **66**(4):556-565. [doi:10.1016/j.jcsr.2009.10.015]

Kaitila, O., 2002. Finite Element Modeling of Cold-Formed Steel Members at High Temperatures. PhD Thesis, Helsinki University, Finland.

Kwon, Y.B., Kim, B.S., Hancock, G.J., 2009. Compression tests of high strength cold-formed steel channels with buckling interaction. *Journal of Constructional Steel Research*, **65**(2):278-289. [doi:10.1016/j.jcsr.2008.07.005]

Papangelis, J.P., Hancock, G.J., 1995. Computer analysis of thin-walled structural members. *Computers and Structures*, **56**(1):157-176. [doi:10.1016/0045-7949(94)00545-E]

Schafer, B.W., 2002. Progress on the Direct Strength Method. Proceeding of 16th International Specialty Conference on Cold-Formed Steel Structures, Orlando, Florida. p.647-662.

Schafer, B.W., Peköz, T., 1998. Direct Strength Prediction of Cold-formed Steel Members Using Numerical Elastic Buckling Solutions. Proceedings of the 14th International Specialty Conference on Cold-Formed Steel Structures, University of Missouri-Rolla, USA, p.69-76.

Sputo, T., Tovar, J., 2005. Application of direct strength method to axially loaded perforated cold-formed steel studs: long wave buckling. *Thin-Walled Structures*, **43**(12):1852-1881. [doi:10.1016/j.tws.2005.08.005]

Tovar, J., Sputo, T., 2005. Application of direct strength method to axially loaded perforated cold-formed steel studs: distortional and local buckling. *Thin-Walled Structures*, **43**(12):1882-1912. [doi:10.1016/j.tws.2005.08.004]

Yan, J., Young, B., 2002. Column test of cold-formed steel channels with complex stiffeners. *Journal of Structural Engineering, ASCE*, **128**(6):737-745. [doi:10.1061/(ASCE)0733-9445(2002)128:6(737)]

Young, B., 2004. Design of channel columns with inclined edge stiffeners. *Journal of Constructional Steel Research*, **60**(2):183-197. [doi:10.1016/j.jcsr.2003.09.001]

Young, B., Rasmussen, K.J.R., 1998. Tests of fixed-ended plain channel columns. *Journal of Structural Engineering, ASCE*, **124**(2):131-139. [doi:10.1061/(ASCE)0733-9445(1998)124:2(131)]

Young, B., Yan, J., 2004a. Channel columns undergoing local, distortional, and overall buckling. *Journal of Structural Engineering, ASCE*, **128**(6):728-736. [doi:10.1061/(ASCE)0733-9445(2002)128:6(728)]

Young, B., Yan, J., 2004b. Design of cold-formed steel channel columns with complex edge stiffeners by direct strength method. *Journal of Structural Engineering, ASCE*, **130**(11):1756-1763. [doi:10.1061/(ASCE)0733-9445(2004)130:11(1756)]

Young, B., Ellobody, E., 2007. Design of cold-formed steel unequal angle compression members. *Thin-walled Structures*, **45**(3):330-338. [doi:10.1016/j.tws.2007.02.015]

Young, B., Chen, J., 2008. Design of cold-formed steel built-up closed sections with intermediate stiffeners. *Journal of Structural Engineering, ASCE*, **134**(5):727-738. [doi:10.1061/(ASCE)0733-9445(2008)134:5(727)]

Yu, C., Schafer, B.W., 2007. Simulation of cold-formed steel beams in local and distortional buckling with applications to the direct strength method. *Journal of Constructional Steel Research*, **63**(5):581-590. [doi:10.1016/j.jcsr.2006.07.008]

Yu, W.W., 2000. Cold-Formed Steel Design (3rd Ed.). Wiley, New York.